Adding an Upper Body to Passive Dynamic Walking Robots by Means of a Bisecting Hip Mechanism

Martijn Wisse, *Member, IEEE*, Daan G. E. Hobbelen, and Arend L. Schwab

Abstract—Passive dynamic walking is a promising idea for the development of simple and efficient two-legged walking robots. One of the difficulties with this concept is the addition of a stable upper body; on the one hand, a passive swing leg motion must be possible, whereas on the other hand, the upper body (an inverted pendulum) must be stabilized via the stance leg. This paper presents a solution to the problem in the form of a bisecting hip mechanism. The mechanism is studied with a simulation model and a prototype based on the concept of passive dynamic walking. The successful walking results of the prototype show that the bisecting hip mechanism forms a powerful ingredient for stable, simple, and efficient bipeds.

Index Terms—Biped, bisecting hip, passive dynamic walking, upper body.

I. INTRODUCTION

TWO-LEGGED walking robots exert a strong attractive appeal due to the resemblance to human beings [1]. Consequently, some major research institutions and private companies have started to develop bipedal (two-legged) robots, which has led to sophisticated machines [2]–[4]. To enable economically viable commercialization (e.g., for entertainment), the challenge is now to reduce the design complexity of these early successes, in search for the ideal set of characteristics: stability, simplicity, and energy efficiency.

A promising idea for the simultaneous reduction of complexity and energy consumption, while maintaining or even increasing the stability, is McGeer's concept of "passive dynamic walking" [5]. On a shallow slope, a system consisting of two legs with well-chosen mass properties can already show stable and sustained walking [6]. No actuators or controls are necessary, as the swing leg moves in its natural frequency. An elegant solution indeed, but thus far, most researchers have only considered the legs.

The addition of an upper body to passive dynamic walkers remains an active research topic. The problem is that the upper body should be stabilized in the upright position, while at the same time, the alternating swing leg should be able to swing passively to a forward position. Some passive solutions have been found [7], [8], in which the upper body is another passive

pendulum-like component. Also, a number of active control solutions have been proposed, such as McGeer's "levered isotonic tendons" [9], variable springs [10], or a controllable "backlash clutch" in the hip joints [11], all fairly complex solutions. In contrast, we have searched for an alternative, mechanical solution.

In this paper, we propose to design the hip joint as a passive bisecting mechanism, similar to that in a pair of compasses. After the background information in Section II, we will first analyze a simple pointmass model in Sections III, IV, and V. Next, Section VI will present the two-dimensional (2-D) simulation model and prototype (Fig. 1) developed for this study. The results of this model and prototype study will be presented in Section VII. Finally, Section VIII will conclude that a bisecting hip mechanism indeed provides an elegantly simple solution for stable and efficient walking with an upper body.

II. BACKGROUND

A. Passive Dynamic Walking

In search for simple, stable, and efficient walking machines, McGeer [5] pioneered the idea of passive dynamic walking, building on work of Mochon and McMahon [13] and Hurmuzlu and Moskowitz [14]. The concept is analogous to the approach of the Wright Brothers to flying; first they mastered motorless gliding until they had a design that was intrinsically stable, could be manually controlled, and glided with only a small descent angle (i.e., could travel far on little gravitational energy). Similarly, McGeer focused on finding a completely passive construction that could walk stably and efficiently, requiring only a minimal downward slope in the walking surface. With dynamic simulations, and based on the method of Poincaré mapping, he analyzed the stability of such walkers, and subsequently built increasingly complex prototypes, the most advanced of which had two legs with knees [Fig. 2(a)]. With symmetrically paired legs, its motions were confined to two dimensions, a solution also adhered to in this paper. Since McGeer's work, the idea of passive dynamic walking has gained in popularity [15]–[18]. The most advanced fully passive walker yet, constructed at Cornell University (Ithaca, NY), has two legs (genuine 3-D dynamics) with knees, and counterswinging arms [see Fig. 2(b)] [6]. It has no upper body.

B. Hip Actuation for Stability

The purely passive walking prototypes demonstrate convincing walking patterns. However, all prototypes require a smooth and well-adjusted walking surface. A small disturbance

The authors are with the Department of Mechanical Engineering, Delft University of Technology, 2628 CD Delft, The Netherlands (e-mail: m.wisse@tudelft.nl).
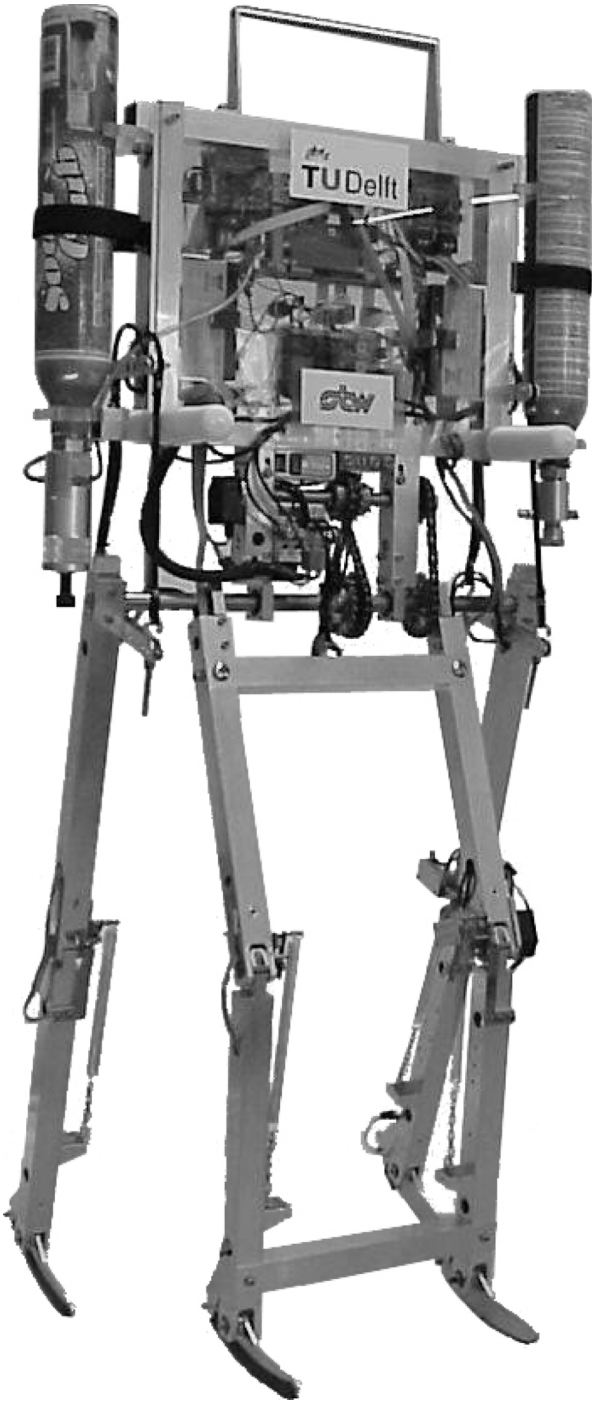
Fig. 1. Prototype "Max" [12]; a 2-D passive dynamic walking robot with an upper body connected to a bisecting mechanism at the hip.
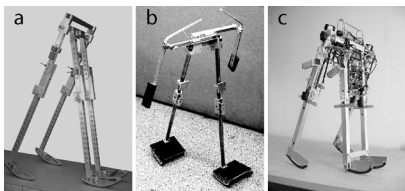

Fig. 2. Previous walkers. (a) Garcia's copy [19] of McGeer's 2-D walker with knees [20], at Cornell University. (b) Fully passive 3-D walker with knees and arms by Collins [6], also at Cornell University. (c) Kneed walker with hip actuation [21], at Delft University of Technology.

(e.g., from small errors introduced with a manual launch) can still be handled, but larger disturbances quickly lead to a failure [22]. 2-D models can suffer from three types of failure: collapsing through the stance knee; falling backward; or falling forward. The first type of failure, knee collapse, is related to the ground reaction force. If this force results in a flexing torque in the knee, a knee collapse could occur. The problem is solved by attaching the feet more forward to the shank, and additionally, a knee latch can be installed. The second type of failure, falling backward, is related to the fluctuations in kinetic and potential energy. In the extreme situation of a robot with point feet, the robot's center of mass (COM) would make a circular path with midstance as the apex. A shortage of initial kinetic energy could cause a failure to pass the apex, resulting in a fall backward. The problem is solved by applying arc feet with a reasonably large radius. This leaves us with the third type of failure, falling forward.

Falling forward occurs when the swing leg is not timely moved to a forward position where it can catch the robot in preparation for its next step. The solution to this problem is correspondingly straightforward; the faster the swing leg is swung forward (and then kept there), the more robust the walker is against disturbances. The exact motion of the swing leg is irrelevant. This idea was tested in simulation models and in a prototype [21] [Fig. 2(c)]. We implemented the idea with a variable spring at the hip joint. The stiffness and damping were kept constant, but the equilibrium angle alternated at each step, always pulling the swing leg forward with respect to the stance leg. As a result, the walker could cope with larger disturbances when the hip spring provided more acceleration, the known tradeoff between energy consumption and stability. Note that the prototype in Fig. 2(c) is the direct predecessor of the prototype presented in this paper. In addition, at this point, we would like to clarify that our robot published in [23] was developed later than the prototype in this paper; the order of publication was inadvertently reversed.

III. POINTMASS MODEL WITH UPPER BODY

The goal of this paper is to add an upper body to an (almost) passive walking robot. We start with a simplified model, as earlier described in [24]. This model should be as simple as possible for the sake of a minimal set of parameters, so a natural starting point would be the "simplest walking model" of Garcia *et al.* [25]. The simplest walking model consists of two rigid massless legs, with small pointmasses m_f as feet and a finite pointmass at the frictionless hip joint. For slopes up to 0.015 rad, this model performs a stable walk downhill.

Their model deserves an accordingly simple upper body. A pointmass will do, connected to a rigid, massless stick that rotates around the hip joint (Fig. 3). The upper body is parameterized with body length l_b and body mass m_b. The default parameter values are somewhat arbitrarily chosen to have some relevance to human walking or to future prototypes (Table I). We made the parameter values dimensionless for comparison with other models: all sizes are scaled with the leg length, so that the leg length is 1, and all masses are scaled with the sum of the pelvis mass and the upper body mass, so that the pelvis mass is $1 - m_b$. The foot mass is not included in this sum for reasons
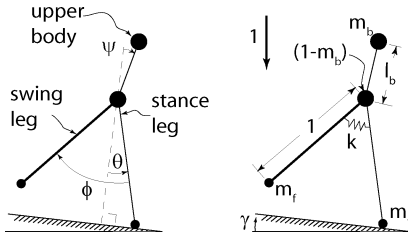
Fig. 3. Model of the simplest walker with upper body; parameters (left) and DOFs (right).

TABLE I
DEFAULT PARAMETER VALUES FOR THE SIMPLEST WALKER WITH UPPER BODY, FROM A ROUGH ESTIMATION OF HUMAN PROPORTIONS. THE PARAMETERS ARE NONDIMENSIONALIZED BY SCALING: MASS IS DIVIDED BY (PELVIS MASS + UPPER BODY MASS), LENGTH IS DIVIDED BY LEG LENGTH, TIME IS DIVIDED BY $\sqrt{\text{leg length/gravity}}$

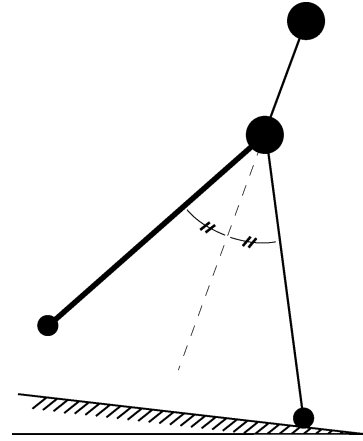| parameter	symbol	human approx.	scaled
Foot mass	m_f	7 kg	0.1
Upper body mass	m_b	49 kg	0.7
(Pelvis mass)	$(1 - m_b)$	21 kg	0.3
Leg length	-	1 m	1
Body length	l_b	0.4 m	0.4
Hip spring stiffness	k		0.4
Slope angle	γ		0.0725 rad

Fig. 4. Kinematic coupling of the upper body to the midway leg angle according to (1).

TABLE II
INITIAL CONDITIONS THAT RESULT IN A CYCLIC WALKING PATTERN FOR THE SIMPLEST WALKER WITH UPPER BODY, USING THE DEFAULT PARAMETER VALUES (TABLE I)

θ_0	0.3821 rad
$(\phi_0 = 2\theta_0)$	(0.7642 rad
$\dot{\theta}_0$	-0.3535 rad/s
$\dot{\phi}_0$	0.0736 rad/s

of compatibility with older models [22]. Time is scaled so that the resulting gravity is 1. There are also two nonhuman parameters: 1) slope angle γ, by which we can tune the walking speed; and 2) hip spring stiffness k, which allows tuning of the step frequency. The spring will turn out to be necessary for stable walking, as will be described in Section V-C. With the default parameter values according to Table I, the model walks with human-like speed and step length, see Section V-A.

As such, the model would have three degrees of freedom (DOFs) (Fig. 3): absolute stance leg angle θ (counterclockwise), relative swing leg angle ϕ (clockwise), and absolute body angle ψ (clockwise). However, the upper body is then just an inverted pendulum jointed around the hip. Without any active control acting on it, one can expect that it will not be kept upright passively. To keep a fully passive upper body upright, A. Ruina (personal communication) suggests four possibilities.

1) Use a light upper body that has its actual COM *below* the hip. This option is not very useful in realistic prototypes.
2) Use springs that keep the upper body upright [10]. This also has the utility that it should give more efficient walking by making the steps smaller at a given speed [18].
3) Use a compass mechanism: a kinematic coupling that keeps the body midway between the two legs (Fig. 4).
4) Keep the model as is, and hope that for some special mass distribution, a stable gait suddenly emerges.

Intuitively, option three is most promising because the number of DOFs is reduced, which improves the chances of finding stable walking cycles. Human beings do not have such a kinematic coupling, but the assembly of pelvic muscles and reflexes could possibly perform a similar function. Also, such a construction can be found in certain reciprocating gait orthoses

[26]. In robot prototypes, such a kinematic coupling can be easily realized. In the model, it is introduced according to

$$\psi = \frac{\phi}{2} - \theta. \tag{1}$$

The other options could provide valuable results, although the first is not interesting as a model for human walking. We intend to investigate options two and four in the future, but in this paper, we will focus on the behavior of the model with the compass-like kinematic constraint.

IV. RESULTS OF POINTMASS MODEL

A. Walking Motion

The walking motion is analyzed with the help of the methods described in [22] and [24]. With the default parameter values, the model takes something like a human walking step if started with the initial conditions from Table II. However, due to its quintessential nature, our model shares some typical nonhuman characteristics with Garcia's simplest walking model. First, the feet are no more than points, hence, the application point of the ground contact force is at a fixed location during one step. Second, there are no actuators, so that the model will only walk if placed on a slope. Third, the legs cannot change length, hence, there are not enough DOFs to allow a double support phase.

The step starts and ends immediately after heel strike (Fig. 5). The hip moves forward like an inverted pendulum with an almost constant speed, while at the same time, the swing leg swings to a forward position. Naturally, the kinematic constraint keeps the upper body at the intermediate leg angle. The motion of the swing leg appears to be that of a free pendulum,
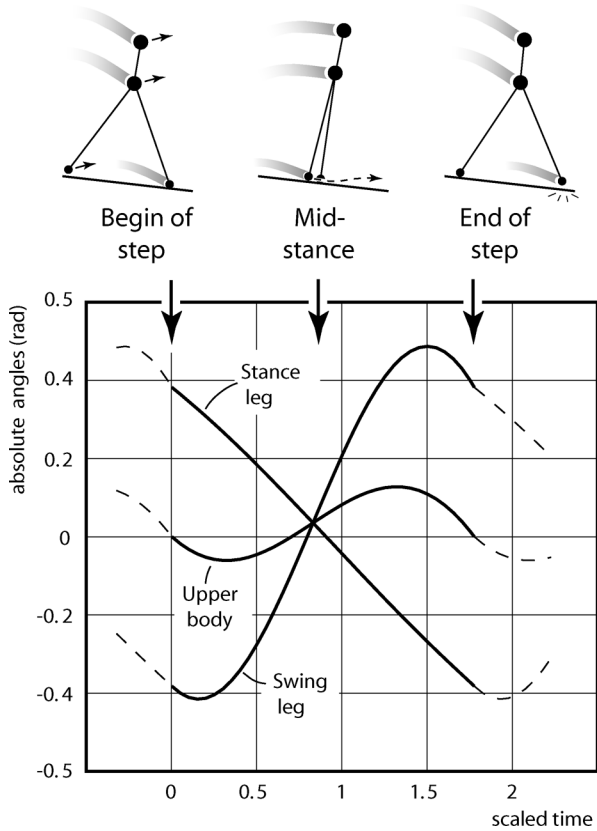
Fig. 5. Cyclic walking motion of the model with upper body. Top: stick figure representation. Bottom: absolute angles of stance leg, swing leg, and upper body. The simulation is performed using the default parameter values in Table I.

while actually, it is mainly the result of the dynamics of the upper body and the hip spring.

The trajectories of the various pointmasses are no surprise; the hip moves forward on a circular path (often referred to as "compass gait" [27]), while the swing foot remains close to the floor. The upper body follows a path almost identical to the hip trajectory at a distance l_b above the hip, only slightly smoother at the heel strike discontinuities. There are two peculiarities. First, the hip trajectory equals that of an inverted pendulum, but its speed does not. Due to the influence of the upper body and the hip spring, the speed of the hip is nearly constant, as can be deducted from the nearly constant stance leg velocity in Fig. 5. Second, the swing foot travels briefly below floor level. Inevitable for a 2-D walker with straight legs, we allow this to happen in our simulation. Human beings and our more sophisticated models [28] and prototypes [29] have knees to solve this problem.

With a scaled step length of 0.746 and a scaled step time of 1.77, the model attains a scaled walking velocity of 0.42. Back on a human scale (on earth), this corresponds to 1.3 m/s. The scaled velocity is the same as the familiar Froude number, $\sqrt{v^2/gl}$, where Froude number = 1 represents the maximum walking speed for any biped. At higher speeds, the foot contact force would become negative, so the biped should switch to running or maybe to Groucho walking. With a Froude number of 0.42, our model is well below that boundary, firmly stepping its way but not even close to running.

The energy consumption of the model at this speed is low. This is usually [23] represented in the nondimensional form of specific resistance c

$$c = \frac{E}{mgs} \qquad (2)$$

i.e., the energy consumption E per distance traveled s per unit of weight (= mass m times gravity g). For passive dynamic walkers, the specific resistance is equal to the sine of the slope angle $\sin \gamma$, as gravity is the only means of energy input. So, our model has a specific resistance of 0.0725 at a (scaled) speed of 0.42. This is much more efficient than human beings walking at the same speed with a specific resistance of approximately 0.38 [30], although the comparison is somewhat unfair, as muscle efficiency is unaccounted for. Also, this is much more efficient than the current generation of walking robots.

B. Inherent Stability

To classify the stability of the walking motion, there are two useful but essentially different definitions. First, we can regard stability in its most strict way. The basis is a walking motion in cyclic equilibrium, called a limit cycle; a certain combination of initial conditions (Table II) keeps repeating itself for all subsequent steps. If started slightly away from the limit cycle, the walking motion is stable if the subsequent step is closer to the limit cycle. Note that this local stability requires the existence of a limit cycle, and that only small disturbances are investigated. We found that the model with the parameter values from Table I and started with the initial conditions from Table II is indeed stable for small disturbances.

Second, we can regard the stability of walking in the broadest and most intuitive form: the robot is stable if it does not fall. We can even allow ourselves to use the formally incorrect term *more stable* for a robot that can handle larger disturbances. Note that this global stability does not require the existence of a limit cycle (every step may be different, as long as the robot does not fall), but that it can only be investigated with the costly method of trying out all possible disturbances.

By application of the cell-mapping method [31], we found that the model performs surprisingly well. The model converges to its limit cycle if started with errors as large as 8% on all initial conditions of Table II, compared with 2% for the simplest walking model [22]. For certain combinations of errors, the errors can even be much larger. This is inspected by evaluation of the *basin of attraction* (Fig. 6), the complete set of initial conditions that eventually lead to cyclic walking. For example, the figure shows that cyclic walking with cyclic initial conditions as in Table II emerges, even if the initial step is twice as large, e.g., $\{\theta_0 = 0.75, \dot{\theta}_0 = -0.75, \dot{\phi}_0 = -1\}$.

V. PARAMETER STUDY ON POINTMASS MODEL

A. Slope and Spring Stiffness; Speed and Step Length

As mentioned in Section II, the model has two parameters that are essential to the model's gait: the slope angle and the hip spring stiffness. Together, they determine the step frequency and the step length, thereby also determining the walking velocity.
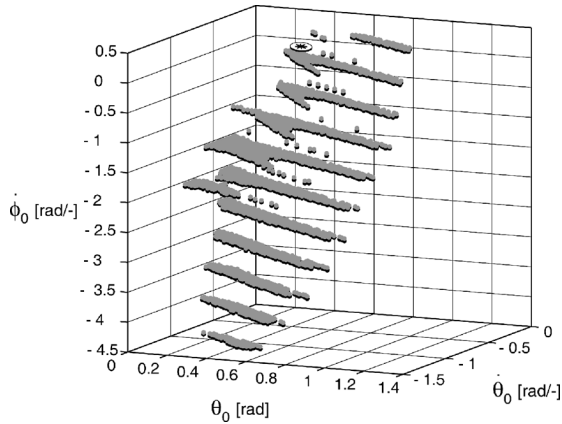
Fig. 6. Basin of attraction of the simplest walking model with upper body. The gray layers of points represent horizontal slices of a 3-D region of initial conditions that eventually lead to the cyclic walking motion. The cyclic motion ($\{\theta_0 = 0.3821, \dot{\theta}_0 = -0.3535, \dot{\phi}_0 = 0.0736\}$, Table II) is indicated with a flat asterisk on a small disk, just above one of the sample slices.

First, for a fixed set of mass and length parameters, the step frequency is mainly determined by the hip spring stiffness. It appears that the swing leg amplitude, step length, slope angle, or walking speed all have a negligible influence on the step frequency [5], [25].

Then, the step length is directly determined by the slope angle; the steeper the slope, the larger the steps. This is a result of the balance between the gravitational energy input and the impulsive energy losses at heel strike. Although a larger step means more energy input, it leads to even more energy loss at heel strike. As a result, the system will automatically converge to a periodic walking motion with a step length that corresponds to the slope angle.

With the hip spring stiffness and the slope angle together, we were able to set both the speed and the step length to human values. It should be noted that these effects are not unique to our model. In fact, Kuo [18] studied these same effects extensively for the simplest walking model to investigate energy matters of human walking.

B. Upper Body Height and Weight

The upper body is parameterized with body length l_b and body mass m_b. The body mass and the pointmass at the pelvis together always sum to 1 for the purpose of scaling, while the body length is scaled to the length of the leg. The default parameters of Table I are chosen so that the model has some relevance to future prototypes. This section investigates the model behavior when the upper body is reduced to nothing or significantly enlarged.

Reduction of the upper body size or mass to zero leads to a model like the simplest walker, except that the simplest walker has no hip spring and an infinitesimally small foot mass. For a very small foot mass, no hip spring is necessary, but for a realistic foot mass, as in Table I, stable walking cycles only exist if a spring is applied. As stated earlier, the hip spring and slope angle together determine the walking speed and the step length. If we set them so that speed and step length match the original model (Table I), we find that the "zero-body-model" needs a

slope angle of $\gamma = 0.147$ rad. In other words, the model with upper body is twice as efficient as the same model without upper body! Apart from that, there is not much difference between the gaits of the two models.

Similarly, an increase in the mass or the size of the upper body will provide an even higher walking efficiency. We found that an increase in m_b has a similar effect as an increase in l_b. As an example, we crudely modeled a person carrying a heavy load on the top of the head by setting $m_b = 0.9$ and $l_b = 1$. The hip spring stiffness and slope angle were again adjusted to obtain human walking speed and step length. The required slope angle is now only $\gamma = 0.0249$ rad; this model walks about three times more efficiently than with the default parameter values! In general, it is clear that the presence of an upper body has a positive influence on the walking efficiency.

The changes of the mass or size of the upper body have little effect on the stability. We investigated the three previously mentioned situations: a) zero upper body mass; b) default parameters (Table I); and c) someone carrying a heavy load on the head ($l_b = 1$, $m_b = 0.9$). In terms of linearized stability, all three situations are stable for small disturbances. In terms of global stability, the allowable errors on all initial conditions are about 8% for all three situations. However, the resultant basins of attraction (as in Fig. 6) have different shapes, so that convergence from larger errors occurs for different combinations of errors. It seems odd that the size or mass of the upper body has no apparent influence on the allowable errors (all 8%), whereas there is such a large difference with the simplest walking model (only 2%). We believe that this is a result of the increased speed and step frequency; the simplest walking model walks slower than our model, which we tuned to walk with human speed. We intend to investigate this effect in the near future.

C. Limits to Stability

Our upper-body walker has a remarkably stable gait if provided with the parameter values from Table I. For certain other parameter values, however, the model has unstable gaits, or even no cyclic walking motions at all. Usually this can be solved by sufficiently increasing the hip spring stiffness k, with a few exceptions. At slopes steeper than $\gamma \approx 0.35$ rad, the equilibrium speed is so high that the stance foot would lose ground contact and the model should start running. The foot mass m_f and the body size and mass l_b and m_b can be chosen arbitrarily small or large; with a high enough value for k, the model still walks fine, although this could result in correspondingly small or large step lengths, which, in turn, could lead to the loss of floor contact.

Inside these boundaries, for each combination of parameter values, there exists a minimal value for k that ensures stability. For the model with the default parameter values of Table I, we studied the effect of variations in k on the cyclic walking motion. For $k > 0.218$ we found steady, stable cyclic walking, as described in Section IV-A. However, for the same value of k, there also exists a second, unstable gait. The steps are shorter and faster, and the motion looks like the model is stumbling forward. McGeer and Garcia discovered this second solution for their models and refer to it as the "short-period gait," as opposed to the normal, stable solution, which is termed "long-period gait." We are only interested in the last type of gait, the
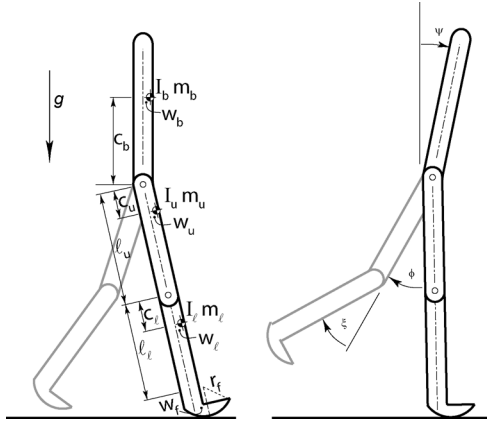
Fig. 7. 2-D five-link model. Left: parameter definition. Right: DOFs (ψ is not measurable in the prototype).

behavior of which we have studied as a function of the parameter value for k.

Above the boundary value, an increase in k results in faster and smaller steps, as discussed in Section IV-A. If we decrease k below 0.218, we cross a bifurcation to asymmetric gaits, first encountering two-period solutions, and for lower k, even higher period solutions. These solutions are still stable. Below $k = 0.162$, we found only unstable gaits, or even no cyclic solutions at all. Garcia found a similar bifurcation to chaos for the simplest walking model when increasing the slope above $\gamma = 0.015$ rad.

We tracked the first bifurcation point over a range of parameter values, because that point represents the minimally required value for k to obtain normal, stable walking. The relation between the minimal value for k and the other parameters is not linear, and there is not an obvious and simple nonlinear relationship. Qualitatively, the required hip spring stiffness k needs to be increased if l_b, m_b, m_f, or γ are increased.

VI. REALISTIC BIPED WITH UPPER BODY

A. Simulation Model

We now move from the pointmass model to a realistic model of a 2-D five-link biped (Fig. 7). The model has a common topology; the upper body is a single rigid link, whereas each leg consists of a thigh and a shank interconnected through a knee joint. The knees are provided with a hyperextension stop (assuming fully inelastic impacts) and a locking mechanism (latch) which is released just after the start of the swing phase. With the bisecting hip mechanism, the total number of DOFs is at most three; absolute upper body angle ψ, interleg angle ϕ, and relative swing knee angle ξ. At the end of a step when the swing knee is fully extended, only two independent DOFs remain (four states; two angles and their velocities). Note that this is the same number of DOFs as for kneed walkers without an upper body [32], due to the constraint of the bisecting hip joint.

Ankle joints are not present, as rigidly attached arc feet have proven to be a simple and sufficient solution for stable passive walking. We assume that the links suffer no flexible deformation and that the joints are free of damping or friction. Also, we assume a perfect bisecting mechanical coupling between the legs and the upper body. The contact between the foot and the

floor is idealized, assuming perfectly circular feet that do not deform or slip, while the heel strike impact is modeled as an instantaneous, fully inelastic impact where no slip and no bounce occurs. The walker walks on level ground, and thus requires a small amount of energy input per step. This is provided by means of the hip muscles, which accelerate the swing leg to a forward position. Their main function is to provide fore–aft stability (cf. Section II-B), but their secondary effect is the input of just enough energy into the system to maintain the cyclic walking motion. Finally, the floor is assumed to be a rigid, flat, and level surface.

B. Simulation Procedure

The simulation procedure is similar to that applied in the pointmass model study of the previous sections. The procedure is a succession of nonlinear numerical dynamic simulations of walking steps which begin and end at the instant immediately after heel strike. Within one step, the equations of motion are numerically integrated until an event is detected, such as knee strike or heel strike, followed by an impact calculation. After the heel strike impact, the simulation of the walking step is ended. The end state of the walker (an instantaneous double stance phase) can then be used as the starting state for the next step, or it can be compared with the initial state of the walker. If the end state equals the initial state, we have found a fixed point representing a cyclic walking motion. We then apply the Poincaré mapping method for stability analysis. Additionally, to investigate how stable the walking motion is, we perform an approximate search for the boundaries of the basin of attraction of the fixed point. For this realistic model, it is unfeasible to do a full investigation of the basin of attraction, so we cannot apply the cell-mapping method, as was done with the pointmass model. Instead, a walking step is simulated with initial conditions that deviate from the fixed point in eight different combinations of states (e.g., a positive deviation on the stance leg angle combined with a negative deviation on the angular velocity of the body). We search for the largest allowable deviations that still lead to successful walking. The resulting estimate for the boundaries of the basin of attraction are a measure for the size of disturbances (at the start of a step) that the walker can still recover from.

C. Default Parameter Values

A set of physically realistic parameter values that lead to stable walking was readily found. Reusing partial designs from previous research [29], we arrived at a 10 kg machine with a 0.6 m leg length and 1.1 m total height. The physical properties, such as the mass distribution, were initially determined by convenient placement of the supplementary electronic and pneumatic components (Section IV). The resultant configuration resulted in stable walking in the simulation, so we have adopted these parameter values as the default values listed in Table III.

D. Construction of the Prototype

The central part of the prototype is its bisecting hip mechanism. Of the many possible forms of implementation, we chose to apply an auxiliary axle connected to the legs with one straight and one cross-over chain (Fig. 8). In hindsight, it is valuable to

TABLE III
DEFAULT PARAMETER VALUES FOR THE PROTOTYPE WITH TWO FULL CO_2 CANISTERS. THE UNDERLINED U, L, AND B SERVE AS SUBSCRIPTS, AS IN FIG. 7

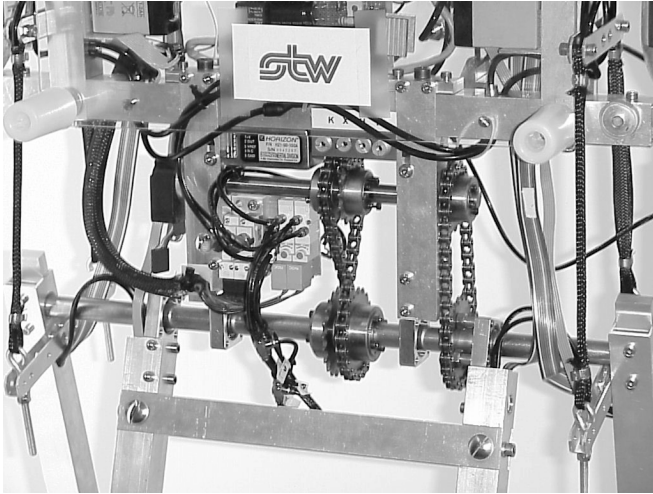|	body	upper leg	lower leg
mass m [kg]	8	0.7	0.7
mom. of Inertia I [kgm^2]	0.11	0.005	0.005
length l [m]	0.45	0.3	0.33
vert. dist. CoM c [m]	0.2	0.15	0.16
hor. offset CoM w [m]	0	0	0
foot radius r_f [m]	-	-	0.25
foot hor. offset w_f [m]	-	-	0.01

Fig. 8. Bisecting hip mechanism in the prototype. The outer legs are rigidly attached to the hip axle, the inner legs can rotate freely. The hip axle is connected through bicycle chains via an auxiliary axle to the inner legs.

report that this solution requires extra attention to the problem of slack in the chains. Also, one must be aware that rather large torques are transmitted through the chainwheels and axles, especially when the prototype occasionally falls. Nonetheless, for our relatively lightweight prototype, this solution is satisfactory. Other possible mechanisms include a four-bar linkage [33], a differential gearbox, or cables and pulleys (as applied in some gait orthoses [26]). Alternatively, the bisecting hip action can also be obtained in fully actuated robots, where a subcontroller maintains the upper body in the bisection angle [34], [35].

The prototype is autonomously powered with an onboard pneumatic system. The pneumatic components are displayed in Fig. 9, clockwise arranged according to the CO_2 flow through the system. The returnable Alco$_2$ jet canister (widely available for home soda machines) contains 450 g CO_2 at the saturation pressure of 5.8 MPa, and weighs 1.2 kg when completely full. The pressure is reduced in two stages, first to approximately 1.2 ± 0.2 MPa and then to 0.6 ± 0.02 MPa. Both levels are manually adjustable. We developed the regulators especially for this project, because they are not commercially available in the required small and lightweight design (the small $40 \times 20 \times 10$ mm block in Fig. 9 actually contains *four* second-stage regulators). The second-stage pressure output is fed via low-power SMC valves to four tiny SMC cylinders that control the knee latches, and to four Shadow McKibben muscles that act as two antagonistic pairs between the robot's body and the outer legs (attached with a moment arm of 60 mm).

Fig. 9. Pneumatic components and a 30 cm ruler to indicate their sizes. The components are clockwise arranged according to the CO_2 flow through the system; 5.8 MPa CO_2 canister, the first-stage pressure regulator to 1.2 MPa, a block of four second-stage regulators to 0.6 MPa, one of four low-power SMC valves, one of four small SMC cylinders, and one of four Shadow McKibben muscles.
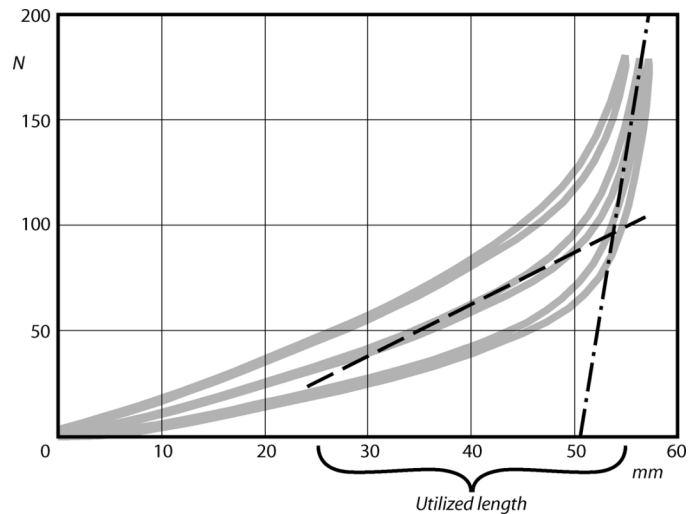

Fig. 10. Muscle force-length diagram at different pressures and the approximation used in the simulations. The dashed line represents one instance of the stiffness (variable with muscle pressure) in the normal operation range, whereas the dash-dotted line models the rigid behavior near maximal extension (invariable). The muscles are mounted with a preload. By their functioning as antagonistic extension stops, a leg can only rotate between -0.35 and $+0.35$ radians with respect to the upper body, so that only a part of the muscle's extension range is used, as indicated in the graph.

The McKibben muscles are an unorthodox choice of actuators. Their characteristics are quite unlike those of the commonly used DC motors and seem disadvantageous at first. They behave like springs with a stiffness proportional to the internal CO_2 pressure (Fig. 10). The use of such muscles is quite energy efficient if they are only required to change pressure once per step, but they are rather unsuitable for continuous control (e.g., to obtain a position servo). The spring behavior is fairly linear for the most part of the 30% extension range, but becomes highly nonlinear near maximal extension, where the stiffness and damping increase dramatically. We modeled this with two stiffnesses, as shown in Fig. 10, together with a high damping ratio near maximal extension. In addition, the CO_2 flow through our pneumatic system to fill the muscles is a slow first-order system with a time constant of $\tau = 0.25$ s. Altogether, the muscles introduce five parameters in the model

that cannot be determined exactly because they are linear approximations of a highly nonlinear behavior, namely, the nominal muscle stiffness, the stiffness near maximal extension, the preload, the damping near maximal extension, and the time constant. We use these parameters to fit the model behavior to the prototype measurements.

Altogether, McKibben muscles do not seem attractive as robot actuators. For the specific task of walking, however, the spring-like behavior, the nonlinearities near maximal extension, and the efficiency when controlled only once per step, together with the low weight and flexibility, make them highly suitable. With these characteristics, the muscles perform three simultaneous tasks.

1) They power the walking motion [36]. A difference of internal pressure between two antagonists results in an asymmetry that pulls forward the swing leg. By alternation of pressures at each step, the muscles inject a small amount of energy into the system, and thus replenishes the energy lost in damping and impacts.
2) They provide robustness against falling forward [21]. Especially, the nonlinear behavior near maximal extension is beneficial for this, as the muscles effectively slow down the forward-rushing swing leg and then keep it in that forward position.
3) They provide the required hip spring stiffness for the upper body (Section V).

Due to this combination of functions, McKibben muscles are a satisfactory choice of actuators for the prototype.

The control system is extremely simple. The prototype has one foot switch underneath the most-right foot, and one underneath one of the middle feet. These two switches are read by a microcontroller, which then triggers only two valve actions per step based on the state of the foot switches. If the inner leg's switch is contacted, the front hip muscles are switched to high pressure and the antagonists to low pressure, effectively pulling the outer legs forward. Simultaneously, the knee latches of the outer legs are released briefly. Then, the system just waits for the outer leg's foot switch to make contact, assuming that knee extension takes place before heel contact. The entire control algorithm is easily implemented in any microcontroller (we have experimented both with a Microchip PIC16f877 and with a LEGO Mindstorms RCX controller).

For postexperiment data analysis, however, a more elaborate electronic system is required. The prototype is equipped with four optical encoders (hip, inner knee, left and right outer knees), and with one gyroscope mounted in the robot's body. The low-level processing (counters and A/D conversion) is still done in a PIC microcontroller, while the data is collected at 50 Hz in a J-stick Java board that can be read out after the experiments. Even with the measurement system active, the entire robot remains fully autonomous.

VII. RESULTS OF REALISTIC BIPED

A. Resultant Motion and Gait Characteristics

The gait of the prototype looks natural, see video at [12]. The resultant walking motion is depicted in Fig. 11, in which
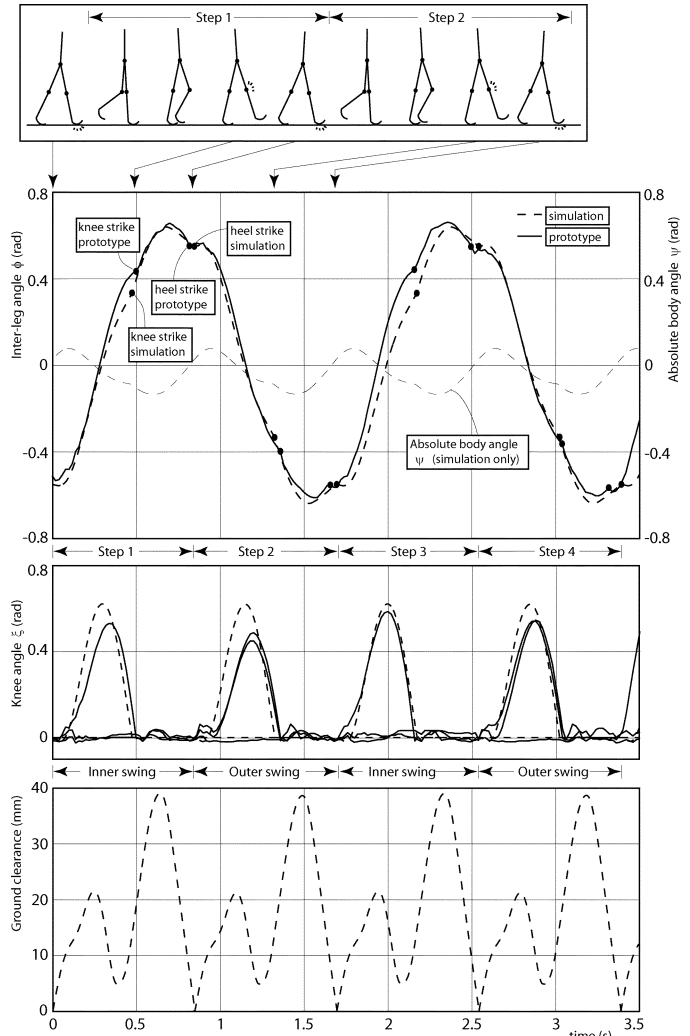

Fig. 11. Comparison of the walking motion of the simulation (dashed lines) and the prototype (solid lines). The absolute body angle ψ and the clearance were not measured in the prototype. The interleg angle shows a slight asymmetry in the prototype's gait. The knees of the prototype show approximately 0.05 rad play of the latch.

we have plotted both the simulation results and the actual prototype recordings. The figure presents the absolute body angle (simulation only, not measured in the prototype), the relative hip angle, and the knee angles as a function of time, together with the foot clearance (also simulation only). The clearance amounts to 5 mm or more throughout the step. The body remains approximately upright with maximal excursions of ± 0.15 rad. The knee reaches full extension 0.5 s after the start of the swing phase. The maximal interleg angle is ± 0.65 rad, but at the time of heel strike, this is ± 0.55 rad, leading to a step length of 0.35 m. The model is walking in its limit cycle, taking 1.2 steps per second, thus walking at 0.42 m/s (Table IV).

The differences between the motions of the model and the prototype are small, especially when considering that the model is walking in its limit cycle, while the prototype is only *close to* its limit cycle, due to constant disturbances; the floor is far from perfectly flat and level. A noticeable difference is in the amount of knee flexion. Especially the knees of the outer legs bend less than predicted by the simulation, probably caused by

TABLE IV
GAIT CHARACTERISTICS WHEN WALKING WITH
THE DEFAULT PARAMETER VALUES

Step length	0.35 m
Step frequency	1.2 Hz
Velocity	0.42 m/s
Nominal clearance	5 mm
Specific resistance	$0.2 \ \mathrm{J/(kgm^2 s^{-2})}$

TABLE V
FIXED POINT VALUES FOR THE THREE INDEPENDENT END STATES JUST
BEFORE HEEL STRIKE, VALID FOR THE PARAMETER VALUES FROM TABLE III.
THE DIFFERENCE BETWEEN SIMULATION AND PROTOTYPE ARISES FROM THE
SIMPLIFIED MODEL FOR THE NONLINEAR MUSCLE BEHAVIOR

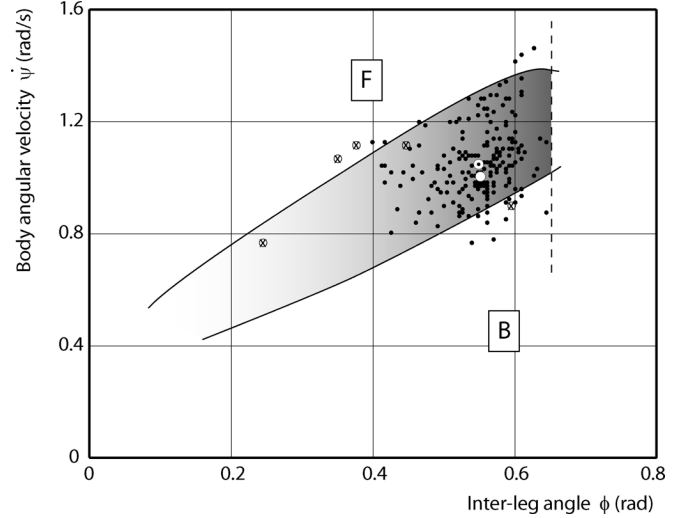|		sim.	proto. (aver. $\pm$s.d.)
Inter-leg angle	ϕ rad	0.55	0.55 $\pm$0.06
Inter-leg ang. vel.	$\dot{\phi}$ rad/s	-0.58	-1.15 $\pm$0.61
Upper body ang. vel.	$\dot{\psi}$ rad/s	1.04	1.03 $\pm$0.17

Fig. 12. Section of the basin of attraction in the Poincaré map. The figure shows the two most sensitive states at the end of a step, namely, the interleg angle ϕ and the angular velocity of the upper body $\dot{\psi}$. The walker is not sensitive to variations in ξ, the third independent end state, which is therefore not shown. The black dots represent 200 measured states during continuous walking, whereas the last step of each series of steps (the last before a fall) is indicated with an encircled "x." The boundaries of the basin of attraction as derived from the simulation are given by the solid black lines. Below the lower boundary, the robot falls backward, above the upper boundary, it falls forward as a result of foot-scuffing. The dashed line represents maximal extension of the hip muscles. Due to the hip actuation, the robot is not likely to arrive in the lower left part of the basin of attraction, but if it did, it would return stably to its limit cycle. The fixed point of the simulation is a white circle, the average measured state is a white circle with a dot.

friction and damping in the knee joint or by a slight delay in the knee latches. The overall effect on the walking motion is small, except for the foot clearance, which then decreases significantly, and indeed, causes most of the failures.

B. Stability

The stability of the cyclic walking motion is usually analyzed by investigating the initial states of each step in a sustained walking motion. We choose to defer from this and to investigate the *end* states instead of the initial states. The difference is that our analysis is based on the velocities just *before* heel strike, in contrast to the tradition of using the velocities just *after* heel strike. The reason is that the velocity measurements in the prototype are unreliable just after an impact, due to transient oscillations in the mechanical system.

At the end of a step, with both feet simultaneously on the floor and with both knees extended, there are only three independent states; interleg angle ϕ, its angular velocity $\dot{\phi}$, and the absolute angular velocity of the body $\dot{\psi}$. Their fixed point values, given in Table V, are determined with the computer simulation for the parameter values in Table III. A Floquet Multiplier analysis of the fixed point on the computer model predicts that the walking motion is stable, i.e., that small errors on the end states in Table V decay step after step.

Fig. 12 shows the walking results of over 200 steps (measured in series of 40 steps, on average) depicted in the phase plane. The graph only represents two out of the three independent states, because the interleg angular velocity $\dot{\phi}$ is not relevant; Table V shows a high variability for this state, and the simulations have shown us that even much larger variations on this state can be allowed without resulting in a failure. The reason for this insensitivity is the fact that the interleg angle is controlled by the hip muscles toward a fixed end position, independent of the initial velocity. The difference between the measured average and the simulated value for $\dot{\phi}$ is a direct result of the simplified model for the muscle nonlinearities at maximal extension.

The experimental results are indicated with black dots in Fig. 12. The last step in a series is indicated with an encircled

cross, because it is the last step before a fall. These experimental results correspond well with the simulation results, which are indicated in the figure with the gray area. According to the simulation model, the gray area is the basin of attraction; a start outside the area will either lead to a fall forward or a fall backward. The average state (indicated in Fig. 12 with a white encircled dot) also corresponds neatly to the fixed point from the simulation model (white circle), see also Table V.

The stability results indicate that the prototype can be easily started with a manual launch (illustrated in Fig. 13). Moreover, we could also realize an automatic launch from a static position, although this only works if the legs are placed with a very small interleg angle, i.e., with the four legs almost all parallel. After a launch, the prototype can walk indefinitely on a level floor until it runs out of power or into a wall. In contrast to the robustness against disturbances in a manual launch, the walker appears to be not too robust against variations in height in the floor surface. The variability of the measurements is quite large. This is a result of the irregularities in the hallway floor. The floor has variations in height of maximally 3.5 mm in one step, amounting to a local slope of $\pm 0.5°$. These irregularities are close to the maximal allowable disturbances as predicted by the simulation model, explaining why some of the measurement points are close to the boundaries of the basin of attraction. The simulation predicts that the walker can handle a step down in the floor of maximally 3 mm. We verified this with an experimental setup where it walked on a rigid, flat, and level surface

Fig. 13. Video stills illustrating the walking motion after a manual launch. Video is available at our website [12].

(not the hallway floor), and then took a step down. Indeed, it could handle not much more than 3 mm.

C. Parameter Sensitivity

The prototype is tolerant to variations in most of the parameters (e.g., 1 kg of extra mass on the upper body has no noticeable effect), except for those parameters that affect the forward velocity. The forward velocity is the net result of the velocity increase during the stance phase and the instantaneous velocity decrease at heel strike. The velocity increase is determined by the amount of time that the robot's COM spends *behind* the foot contact point (deceleration), and the amount of time spent *in front of* the contact point (acceleration). Any parameter that influences these has a strong effect on the walking motion; with too much deceleration, the walker will have a tendency to fall backward, whereas with too much acceleration, the resultant walking velocity will be high, and thus the chances of falling forward increase.

Parameters with a direct influence are w_b, w_u, and w_l (Fig. 7 and Table III), which determine the horizontal position of the COM, and w_f and r_f, which determine the foot contact point. The effect of the position of the COM is strong. For our 10 kg walker, a 500 g additional mass that can be attached up to 100 mm in front or behind the hip joint already provides sufficient tuning possibilities. In our opinion, the automatic control of the fore–aft balance will be one of the major improvements for future dynamic walking robots.

The foot radius r_f determines how much the foot contact point travels forward during the stance phase, and thus a larger radius has a weakening effect on both the robot's deceleration and acceleration. Previous experiments and simulations [29] have shown that this effect is beneficial to the robot's robustness against disturbances. A forward foot offset $w_f > 0$ creates a forward tilt of the entire robot (best visualized in a drawing of the heel strike state), and thus results in faster walking. Therefore, an increase in w_f should be accompanied by a backward displacement of the COM. Note that this observation is only valid for a walker with an upper body with the bisecting hip mechanism and with a substantial mass at a substantial distance

above the hip joint. For walkers without an upper body, the effect is reversed.

The hip actuation has an indirect but significant influence on the deceleration and acceleration during the stance phase. For any walker with physically feasible parameter values (also without upper body), the COM moves forward when the swing leg is swung forward. This is best verified in a simplified analysis without gravity. If the swing leg is moved quickly by a strong hip actuation, then that forward displacement takes place early in the stance phase, and thus, the COM will spend relatively more time in front of the foot contact point. In other words, the faster the swing leg is moved forward, the faster the robot will walk. The strength of this effect depends on the amount of inertia (of both the legs and the upper body) that is involved when the hip actuators are engaged.

There seems to be a counterproductive effect here, as the hip actuation was installed in the first place to *reduce* the chances of falling forward, and now it appears to *increase* that chance by increasing the walking velocity. This can be resolved easily, however, with a backward adjustment of the robot's COM so that the total effect (of hip actuation and mass displacement) is an enlargement of the basin of attraction.

In conclusion, the parameters of the upper body barely influence the walking behavior and the stability. There is almost no effect of an increase of the mass or a vertical displacement of the COM. Only the fore–aft position of the COM is important, as it regulates the average forward walking velocity, and thus the chances of falling forward or backward.

D. Energy Efficiency

The specific cost of transport [(2)] of our prototype is calculated with the CO_2 expansion through the muscles from the 0.6 MPa input pressure to 0.24 MPa relief pressure. The prototype uses 208 mg CO_2 per step (allowing it to walk for 30 min on a single canister). The exergy (or "availability"), i.e., the amount of work that could theoretically be done with gas expanding from 0.6 MPa to 0.24 MPa, is 10.6 J per step, so the specific cost of transport equals 0.32. Although the specific cost of transport for the prototype resembles that of a walking human being, some deliberations must be taken into account.

On the one hand, one could argue that the prototype is much more efficient than the human. The pneumatic muscles are not optimal for their task, because they have a fairly large "dead volume" which must pressurized at each action cycle. They use much more pneumatic energy than the amount of work they produce. We determined with the simulation model that the amount of work produced by the muscles (i.e., their force integrated over their elongation) is only 0.5 J per step, leading to a very low specific cost of transport of 0.01. Note that this value is in the same range of the fully passive walkers as in Fig. 2(a) and (b).

On the other hand, one could argue that the prototype is much less efficient than the human. The specific cost of transport for the human includes the metabolic cost of the entire system, and specifies how well the available energy is used. In that respect, it would be fairer for the prototype calculations to also include the idle pressure reduction from 5.8 to 0.6 MPa. Although exact figures are not available, it is certain that the total amount of available pneumatic energy from the CO_2 canister is factors higher

than the energy that is used in the muscles. However, the main cause of this apparent waste of available energy is not in the applied concept of passive dynamic walking, but rather in the unavailability of pneumatic components that can use the energy of the high-pressure canister. It is expected that ongoing research in the field of pneumatics will eventually solve this problem.

VIII. CONCLUSION

This paper reports on the successful addition of an upper body to a walking robot based on the concept of passive dynamic walking. The upper body is connected to the legs by means of a bisecting hip mechanism which forms a passive solution to stabilize the upper body, while simultaneously allowing a passive swing leg motion. The prototype walks stably and efficiently. The fore–aft position of the COM of the upper body is a powerful parameter for the stability of the walking motion. Conversely, the height of the COM, the total mass, and the mass distribution have no noticeable influence on the performance. Thus, we conclude that the bisecting hip mechanism forms a practical and simple solution to construct efficient bipedal walking robots, in agreement with the concept of passive dynamic walking.

The simulation results suggest that the capability to reject larger disturbances increases when the model walks faster. So far, this effect seems to be unrelated to the added upper body. It is an interesting effect that we intend to research in the near future.

REFERENCES

[1] R. Regele, W. Bott, and P. Levi, "Prorobot—Predictions for the future development of humanoid robots," in *Autonome Mobile Systeme*, R. Dillmann, H. Wörn, and T. Gockel, Eds. Berlin, Germany: Springer, 2003, pp. 292–303.

[2] F. Pfeiffer, K. Löffler, and M. Gienger, "The concept of jogging johnnie," in *Proc. IEEE Int. Conf. Robot. Autom.*, Washington, DC, May 2002, pp. 3129–3135.

[3] Y. Sakagami, R. Watanabe, C. Aoyama, S. Matsunaga, N. Higaki, and M. Fujita, "The intelligent asimo: System overview and integration," in *Proc. Int. Conf. Intell. Robots Syst.*, Lausanne, Switzerland, Sep. 30–Oct. 4, 2002, pp. 2478–2483.

[4] Y. Kuroki, M. Fujita, T. Ishida, K. Nagasaka, and J. Yamaguchi, "A small biped entertainment robot exploring attractive applications," in *Proc. IEEE Int. Conf. Robot. Autom.*, Taipei, Taiwan, R.O.C., Sep. 2003, pp. 471–476.

[5] T. McGeer, "Passive dynamic walking," *Int. J. Robot. Res.*, vol. 9, no. 2, pp. 62–82, Apr. 1990.

[6] S. H. Collins, M. Wisse, and A. Ruina, "A two-legged kneed passive dynamic walking robot," *Int. J. Robot. Res.*, vol. 20, no. 7, pp. 607–615, Jul. 2001.

[7] E. Borzova and Y. Hurmuzlu, "Passively walking five link robot," *Automatica*, vol. 40, no. 4, pp. 621–629, 2004.

[8] M. W. Gomes and A. Ruina, "A walking model with no energy cost," *Phys. Rev. E.*, to be published.

[9] T. McGeer, R. Chatila and G. Hirzinger, Eds., "Passive dynamic biped catalogue," in *Proc. Exp. Robot. II: 2nd Int. Symp.*, Berlin, Germany, 1992, pp. 465–490.

[10] R. Q. van der Linde, "Bipedal walking with active springs, gait synthesis and prototype design," Ph.D. dissertation, Delft Univ. Technol., Delft, The Netherlands, 2001.

[11] M. Okada, T. Shinohara, T. Gotoh, S. Ban, and Y. Nakamura, "Double spherical joint and backlash clutch for lower limbs of humanoids," in *Proc. IEEE Int. Conf. Robot. Autom.*, 2003, pp. 491–496.

[12] In our list of prototypes on the website, look for the robot with the name Max, [Online]. Available: http://www.dbl.tudelft.nl/

[13] S. Mochon and T. A. McMahon, "Ballistic walking," *J. Biomech.*, vol. 13, pp. 49–57, 1980.

[14] Y. Hurmuzlu and G. D. Moskowitz, "Bipedal locomotion stabilized by impact and switching: I. Two and three dimensional, three elements models, II. Structural stability analysis of a four element bipedal locomotion model," *Dyn. Stability Syst.*, vol. 2, no. 2, pp. 73–112, 1987.

[15] A. Goswami, B. Thuilot, and B. Espiau, "A study of the passive gait of a compass-like biped robot: Symmetry and chaos," *Int. J. Robot. Res.*, vol. 17, no. 12, pp. 1282–1301, Dec. 1998.

[16] P. T. Piiroinen, "Recurrent dynamics of nonsmooth systems with application to human gait," Ph.D. dissertation, Royal Inst. Technol., Stockholm, Sweden, 2002.

[17] J. E. Pratt, "Exploiting inherent robustness and natural dynamics in the control of bipedal walking robots," Ph.D. dissertation, Mass. Inst. Technol., Cambridge, MA, 2000.

[18] A. D. Kuo, "Energetics of actively powered locomotion using the simplest walking model," *J. Biomech. Eng.*, vol. 124, pp. 113–120, Feb. 2002.

[19] M. Garcia, A. Chatterjee, and A. Ruina, "Efficiency, speed, and scaling of two-dimensional passive-dynamic walking," *Dyn. Stability Syst.*, vol. 15, no. 2, pp. 75–99, 2000.

[20] T. McGeer, "Passive walking with knees," in *Proc. IEEE Int. Conf. Robot. Autom.*, Los Alamitos, CA, 1990, pp. 1640–1645.

[21] M. Wisse, A. L. Schwab, R. Q. van der Linde, and F. C. T. van der Helm, "How to keep from falling forward: Elementary swing leg action for passive dynamic walkers," *IEEE Trans. Robot.*, vol. 21, no. 3, pp. 393–401, Jun. 2005.

[22] A. L. Schwab and M. Wisse, "Basin of attraction of the simplest walking model," in *Proc. ASME Des. Eng. Tech. Conf.*, Pittsburgh, PA, 2001, DETC2001/VIB-21363.

[23] S. H. Collins, A. Ruina, R. L. Tedrake, and M. Wisse, "Efficient bipedal robots based on passive-dynamic walkers," *Science*, vol. 307, pp. 1082–1085, Feb. 2005.

[24] M. Wisse, A. L. Schwab, and F. C. T. van der Helm, "Passive dynamic walking model with upper body," *Robotica*, vol. 22, pp. 681–688, 2004.

[25] M. Garcia, A. Chatterjee, A. Ruina, and M. J. Coleman, "The simplest walking model: Stability, complexity, and scaling," *ASME J. Biomech. Eng.*, vol. 120, no. 2, pp. 281–288, Apr. 1998.

[26] M. J. Ijzerman, G. Baardman, H. J. Hermens, P. H. Veltink, H. B. K. Boom, and G. Zilvold, "The influence of the reciprocal cable linkage in the advanced reciprocating gait orthosis on paraplegic gait performance," *Prosthetics Orthotics Int.*, vol. 21, pp. 52–61, 1997.

[27] V. T. Inman, H. J. Ralston, and F. Todd, *Human Walking*. Baltimore, MD: Williams & Wilkins, 1981.

[28] M. Wisse and A. L. Schwab, "A 3D passive dynamic biped with roll and yaw compensation," *Robotica*, vol. 19, pp. 275–284, 2001.

[29] M. Wisse and J. van Frankenhuyzen, "Design and construction of Mike; A 2D a autonomous biped based on passive dynamic walking," in *Adaptive Motion of Animals and Machines*, H. Kimura and K. Tsuchiya, Eds. Tokyo, Japan: Springer-Verlag, 2006, pp. 143–154.

[30] H. J. Ralston, "Energy-speed relation and optimal speed during level walking," *Int. z. Angew. Physiol.*, vol. 17, pp. 277–283, 1958.

[31] C. S. Hsu, *Cell-to-Cell Mapping; A Method of Global Analysis for Nonlinear Systems*. New York: Springer, 1987, vol. 64, Appl. Math. Sci..

[32] M. Garcia, A. Chatterjee, and A. Ruina, "Speed, efficiency, and stability of small-slope 2D passive-dynamic bipedal walking," in *Proc. IEEE Int. Conf. Robot. Autom.*, Piscataway, NJ, 1998, pp. 2351–2356.

[33] S. H. Collins and A. Ruina, "A bipedal walking robot with efficient and human-like gait," in *Proc. IEEE Int. Conf. Robot. Autom.*, Barcelona, Spain, 2005, pp. 1983–1988.

[34] J. E. Pratt, C.-M. Chew, A. Torres, P. Dilworth, and G. Pratt, "Virtual model control: An intuitive approach for bipedal locomotion," *Int. J. Robot. Res.*, vol. 20, no. 2, pp. 129–143, 2001.

[35] C. Chevallereau, G. Abba, Y. Aoustin, F. Plestan, E. R. Westervelt, C. Canudas de Wit, and J. W. Grizzle, "Rabbit: A testbed for advanced control theory," *IEEE Control Syst. Mag.*, vol. 23, no. 5, pp. 57–79, Oct. 2003.

[36] R. Q. van der Linde, "Design, analysis and control of a low power joint for walking robots, by phasic activation of McKibben muscles," *IEEE Trans. Robot. Autom.*, vol. 15, no. 4, pp. 599–604, Aug. 1999.

Martijn Wisse (M'02) received the M.S. and Ph.D. degrees in mechanical engineering from Delft University of Technology, Delft, The Netherlands, in 2000 and 2004, respectively.

He is currently an Assistant Professor with Delft University of Technology in Humanoid Robotics.

Arend L. Schwab received the M.S. and Ph.D. degrees in mechanical engineering from Delft University of Technology, Delft, The Netherlands, in 1983 and 2002, respectively.

He has been an Assistant Professor with Delft University of Technology since 1983. In 2002–2003, he was a Visiting Professor at Cornell University's Department of Theoretical and Applied Mechanics, Ithaca, NY. His research interests include multibody dynamics, contact phenomena like nonholonomics and collisions, flexible multibody systems, finite element method, legged locomotion, and bicycle dynamics.

Daan G. E. Hobbelen received the M.Sc. degree with honors in mechanical engineering in 2003 from the Delft University of Technology, Delft, The Netherlands, where he is currently working toward the Ph.D. degree.